Paramecium Calmodulin Mutants Defective in Ion Channel Regulation Can Bind Calcium and Undergo Calcium-Induced Conformational Switching†

Olav R. Jaren, Shawn Harmon, Arthur F. Chen, and Madeline A. Shea*

Department of Biochemistry, University of Iowa College of Medicine, Iowa City, Iowa 52242-1109

Received January 7, 2000; Revised Manuscript Received April 12, 2000

ABSTRACT: Calmodulin (CaM) is an essential eukaryotic protein that binds calcium ions cooperatively at four EF-hand binding sites to regulate signal transduction pathways. Interactions between the apo domains of vertebrate CaM reduce the calcium affinities of sites I and II below their intrinsic values, allowing sequential opening of the two hydrophobic clefts in CaM. Viable domain-specific mutants of *Paramecium* calmodulin (PCaM) differentially affect ion channels and provide a unique opportunity to dissect the roles of the two highly homologous half-molecule domains. Calcium binding induced an increase in the level of ordered secondary structure and a decrease in Stokes radius in these mutants; such changes were identical in direction to those of wild type CaM, but the magnitude depended on the mutation. Calcium titrations monitored by changes in the intrinsic fluorescence of Y138 in site IV showed that the affinities of sites III and IV of wild type PCaM were (i) higher than those of the same sites in rat CaM, (ii) equivalent to those of the same sites in PCaM mutants altered between sites I and II, and (iii) higher than those of PCaM mutants modified in sites III and IV. Thus, calcium saturation drove all mutants to undergo conformational switching in the same direction but not to the same extent as wild type PCaM. The disruption of the allosteric mechanism that is manifest as faulty channel regulation may be explained by altered properties of switching among the 14 possible partially saturated species of PCaM rather than by an inability to adopt two end-state conformations or target interactions similar to those of the wild type protein.

Calmodulin (CaM) is a protein essential in neuronal signaling, muscle contraction, fertility, metabolism, and other fundamental physiological processes. It has 148 amino acids with four EF-hand calcium binding sites. These sites are organized as cooperative pairs in each half-molecule domain (N-domain, residues 1−75; C-domain, residues 76−148). The four EF-hand motifs apparently arose from two gene duplication events giving a sequence (Figure 1) that has the repetitive organization represented by an alternating sequence of segments (α−β−α′−β′). Although it is the same size as myoglobin, its functional organization is like that of hemoglobin (a dimer of dimers).

Cooperative binding of four calcium ions to CaM (sites I−IV) causes large conformational changes that control its activation of enzymes and structural proteins (Figure 2). Each half-molecule domain consists of a four-helix bundle that opens a hydrophobic cleft upon calcium binding. For two decades, the dominant view of activation has been of a two-state process: the fully calcium-saturated state is "on" and the calcium-depleted (or apo) state is "off". There are a few targets (e.g., neuromodulin) that are known to function "in reverse": to bind preferentially to the apo state of CaM and to release it upon calcium binding.

Accounting for the unique sequence of each of the four sites, 16 possible states are found along the pathway of binding calcium to this monomeric allosteric protein. These are represented below, where a dash indicates a vacant site and a dot indicates a calcium ion. In wild type CaM of organisms other than yeast, the sites fill sequentially with III and IV having an approximately 10-fold higher affinity for calcium than sites I and II. This is a conundrum because of the high degree of sequence homology among sites (Figure 1).

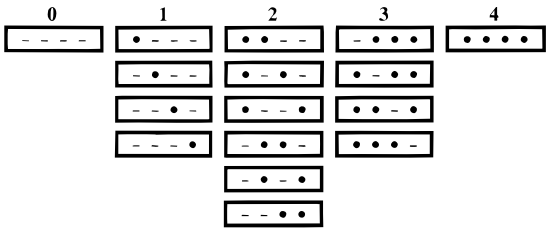

Although there are 16 states, not all of these are populated to an equivalent degree during the course of a calcium gradient. However, it is difficult experimentally to resolve the properties of individual states along a cooperative pathway because intermediates are rarely abundant and their conformational properties may be indistinguishable from those of other intermediate states. Because CaM is essential for eukaryotes, it also is difficult to isolate functional mutants that reveal the mechanism of its allostery.

From stoichiometric calcium titrations of vertebrate CaM monitored by NMR (*1*), it has been clear for more than a decade that a half-saturated state with sites III and IV occupied and sites I and II vacant was a populated conformation

† These studies were supported by an award from the National Institutes of Health (R01 GM 57001) to M.A.S. and an American Heart Predoctoral Fellowship to O.R.J.

* Corresponding author. Telephone: (319) 335-7885. E-mail: madeline-shea@uiowa.edu.

10.1021/bi000037w CCC: $19.00
Published on Web 05/18/2000

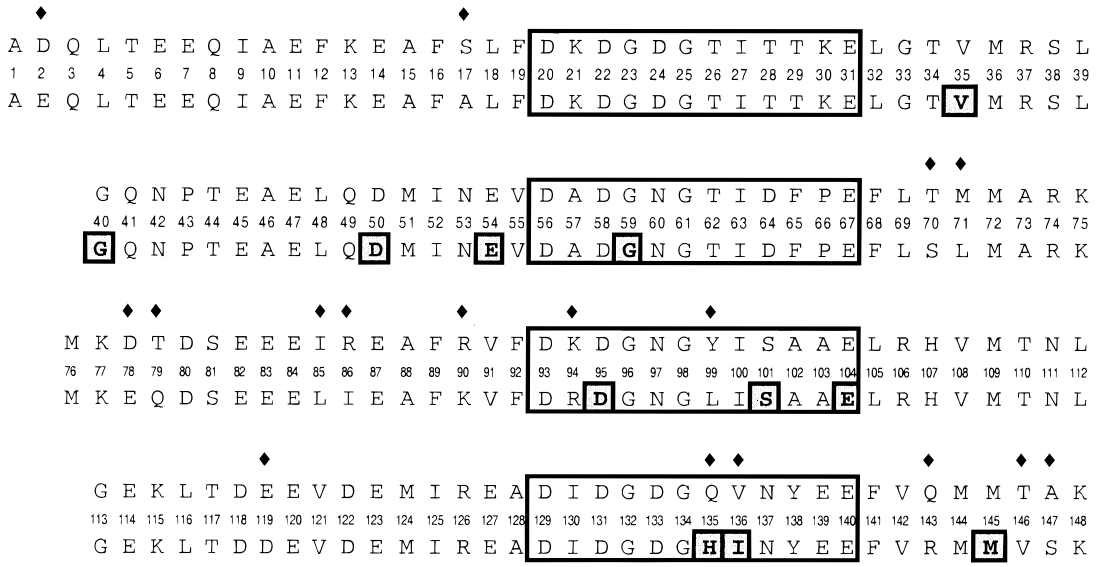

FIGURE 1: Alignment of rat CaM (top) and *Paramecium* CaM (bottom) amino acid sequences; calcium binding sites are aligned and enclosed in boxes. Black diamonds indicate sites of sequence divergence between the two species; there are 17 total sequence differences. Small boxes indicate positions of mutations in PCaM.

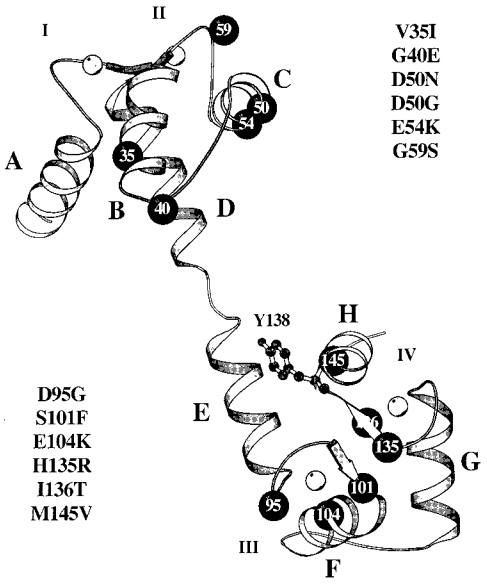

FIGURE 2: Ribbon diagram of the α-carbon backbone of $(Ca^{2+})_4$−PCaM (1osa) made with the program Molscript (*51*). Calmodulin contains four EF-hand motifs. The eight helices are lettered in alphabetical order (A−H) from the amino terminus. Calcium ions are shown as gray spheres, and the calcium binding sites are labeled I−IV. Sites of mutations are marked by black spheres on the backbone and numbered by their position in the sequence; amino acid substitutions are indicated by the labels.

between the apo and fully saturated states. Subsequent studies have shown that affinity differences and interdomain interactions are responsible for the 10-fold separation in calcium affinity between apparently homologous domains that leads to this sequential filling of the two pairs of sites. Although the molecular mechanism for coupling is not understood, proteolytic footprinting titrations of rat CaM have shown that helix B (bracketing site I in the N-domain; see Figure 2) responds to calcium binding at sites III and IV in the C-domain (*2*−*4*).

Studies of the cloned and overexpressed half-molecule fragments of rat CaM showed that the intrinsic affinities of the two domains were very close (*4*). Thermal denaturation of these same half-molecule fragments monitored by CD[1] showed that the apo N-domain is intrinsically more stable than the apo C-domain and that the unfolding of the full-length protein was best described by a three-state transition in which neither of the unfolding processes corresponded precisely to the isolated fragments. However, these studies did not identify the pathway of energetic coupling between the domains. Studies using computations (*5*) and fluorescence spectroscopy (*6*) have attempted to dissect the roles of individual amino acids in this important transition. Site-specific mutagenic studies to corroborate postulated pathways of domain coupling have not shown large effects (*7*). Thus, it is a surprise that mutations in individual calmodulin domains correlate with defects in the activation of different ion channels (*8*, *9*).

These unusual mutants were identified by Kung and co-workers who screened randomly generated mutants of *Paramecium* and found two populations of organisms defective in stimulus response as evidenced by unusual swimming behavior (*8*). These phenotypes were traced unexpectedly to mutations in the gene for CaM and were found to segregate by domain. Mutations in the N-domain of *Paramecium* CaM (PCaM) decreased the calcium-dependent sodium current (the phenotype was under-reaction to a stimulus), while mutations in the C-domain decreased the calcium-dependent potassium current (the phenotype was over-reaction to a stimulus). Furthermore, within each domain, the distribution of mutations was not random (Figure 1). Mutations in the N-domain of PCaM clustered *between* calcium binding sites I and II (i.e., in helices B and C), while mutations in the C-domain clustered *within* calcium binding sites III and IV (*8*, *9*).

These findings were the first demonstration of calmodulin mutants with domain-specific physiological effects and raised many questions about the redundancy of the roles of the domains in CaM. Subsequent studies of yeast CaM using

[1] Abbreviations: PCaM, *Paramecium* calmodulin; CD, circular dichroism; EGTA, ethylene glycol bis(2-aminoethyl ether)-*N*,*N*,*N*′,*N*′-tetraacetic acid; NTA, nitrilotriacetic acid; pCa, $-RT \log[Ca^{2+}]_{free}$; R_s, Stokes radius.

alanine-scanning mutagenesis showed a similar division of effects on physiological processes (*10*, *11*). Because the sequence of PCaM is 88% identical to that of rat CaM (Figure 1), these viable but deleterious mutations of PCaM can provide unique insights into the allosteric mechanism of calcium binding to calmodulin in vertebrates.

Reflecting on the positions of the mutated residues and the role of helix B in interdomain coupling of sites III and IV to sites I and II, we hypothesize that mutations in the C-domain primarily affect the intrinsic calcium affinities of sites III and IV while mutations in the N-domain affect interdomain interactions or the intrinsic calcium affinities of sites I and II. Thus, recognition and binding of target proteins by PCaM will depend on both the intrinsic calcium affinities of the sites and domain−domain interactions (i.e., all determinants of the order of filling the sites). Some of these mutants may have normal responses to calcium but be defective only because of domain-specific alterations in surface contacts with the target protein.

This is the first report of biophysical studies to probe the molecular defects that lead to dysfunctional calcium activation of both sets of mutant PCaM sequences. The goal of this study was to determine whether any or all of these mutants of PCaM (1) undergo normal calcium-induced conformational switching (i.e., analogous in direction and magnitude to that of wild type PCaM) and (2) bind calcium with the same affinity at sites III and IV (in the C-domain). To resolve these two issues, the mutants were studied using optical spectroscopy (UV−vis, fluorescence, and CD) and a hydrodynamic method (analytical gel permeation chromatography). The studies reported here were conducted in the absence of target molecules to determine the fundamental flaws in the switching properties of each mutant protein.

MATERIALS AND METHODS

Purification of Calmodulin. Routine laboratory chemicals were of the highest grade commercially available. Difluoro-BAPTA was purchased from Molecular Probes (Eugene, OR). Bacterial overexpression vectors for recombinant *Paramecium* calmodulin (wild type and 12 mutants) in JM-109 cells were a gift from C. Kung (University of Wisconsin, Madison, WI). Purification of calmodulin from bacterial cells followed that of Putkey (*12*) with a slight modification of using 10 mM $CaCl_2$ in the calcium-containing buffers to account for the lower calcium binding affinity of some mutants. Recombinant calmodulin samples were purified to approximately 97−99% purity as judged by silver nitrate staining of overloaded reducing SDS−PAGE, small zone chromatography on a Superdex75 column (Pharmacia), and reversed phase HPLC. Purified CaM was dialyzed at 5° into a buffer of 50 mM HEPES, 100 mM KCl at pH 7.40 and 22 °C. Aliquots were stored at −20 °C; concentrations were determined using the BCA protein assay (Pierce, Rockford, IL) calibrated by comparison with UV spectra and amino acid analysis. Multiple preparations of each mutant were used over the course of the study.

UV Spectroscopy. Spectra were collected with an Aviv 14DS spectrophotometer using a quartz cuvette with a 1 cm path length. Calcium was removed by the addition of 0.39 mM EGTA in 50 mM HEPES and 95.5 mM KCl at pH 7.40 and 22 ± 1 °C. PCaM was then calcium-saturated by the addition of $CaCl_2$ to a final concentration of 0.95 mM. A representative pair of spectra for wild type PCaM is shown in Figure 3.

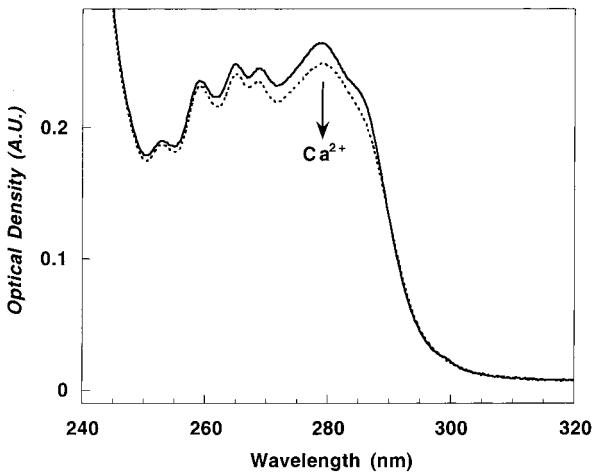

FIGURE 3: UV spectra of apo and Ca^{2+}-saturated wild type PCaM, 50 mM HEPES, 100 mM KCl, and 60 μM CaM at pH 7.40 and 22 °C.

Table 1: Stokes Radii and Ellipticity Changes of Apo and Calcium-Saturated PCaM

protein	R_s (Å) apo PCaM	R_s (Å) Ca-saturated PCaM	ΔR_s	$\Delta\theta_{222}$ (%)
WT	25.41 ± 0.25	24.12 ± 0.11	1.29	12.2 ± 1.4
V35I/D50N	24.94 ± 0.32	23.91 ± 0.20	1.03	11.3 ± 0.8
G40E	25.81 ± 0.35	24.43 ± 0.20	1.38	13.5 ± 0.7
G40E/D50N	25.61 ± 0.13	23.91 ± 0.33	1.70	14.6 ± 1.1
D50G	25.43 ± 0.22	23.86 ± 0.15	1.57	12.6 ± 0.1
E54K	24.91 ± 0.25	24.10 ± 0.07	0.81	10.8 ± 0.4
G59S	25.60 ± 0.05	24.38 ± 0.28	1.22	13.5 ± 1.1
D95G	25.40 ± 0.17	24.23 ± 0.22	1.17	11.1 ± 1.5
S101F	25.52 ± 0.04	23.95 ± 0.06	1.57	15.4 ± 0.4
E104K	25.56 ± 0.06	23.61 ± 0.23	1.95	7.2 ± 0.5
H135R	25.36 ± 0.05	24.12 ± 0.09	1.24	12.5 ± 0.8
I136T	27.25 ± 0.40	24.21 ± 0.03	3.04	33.0 ± 1.5
M145V	25.48 ± 0.13	23.93 ± 0.19	1.55	14.0 ± 0.3
average[a]	25.56 ± 0.57	24.06 ± 0.23		

[a] Averages of Stokes radii for WT and 12 mutants and standard deviations of that distribution are reported without propagation of error for individual mutants.

Circular Dichroism. Spectra were recorded from 260 to 210 nm using an Aviv 62DS instrument with a 1 cm path length quartz cuvette; 6−10 replicates of each protein were conducted. Spectra of apo PCaM were collected in 2 mM HEPES, 100 mM KCl, and 200 μM EGTA at pH 7.40 and 22 °C. Spectra of calcium-saturated PCaM were recorded after calcium was added to a final concentration of 3.3 mM. Calcium-induced changes in ellipticity at 222 nm ($\Delta\theta_{222}$) were calculated by normalizing $\theta_{222}^{calcium}$, the ellipticity of a calcium-saturated protein, to the value of θ_{250} of the same protein under apo conditions [i.e., $\Delta\theta_{222} = (\theta_{222}^{calcium} - \theta_{250}^{apo})/(\theta_{222}^{apo} - \theta_{250}^{apo})$, with the fraction reported as a percentage in Table 1].

Stokes Radius. Analytical gel permeation chromatography (*7*) was used to determine calcium-dependent changes in the Stokes radius (R_s) of wild type and mutant PCaM samples. The values represented in Figure 4 were derived from 6−10 replicates for each protein sample using an FPLC and Superdex75 column (Pharmacia). Apo conditions included 50 mM HEPES, 100 mM KCl, 0.5 mM NTA, and 0.5 mM

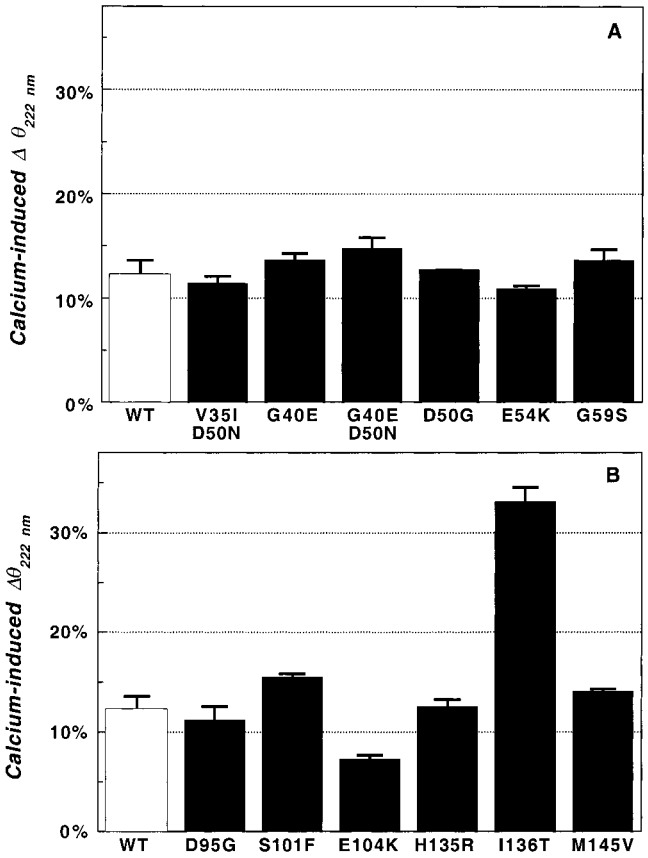

FIGURE 4: Changes in θ_{222} from apo to calcium-saturating conditions. Values for WT PCaM are shown by white bars, and mutant values are shown by black bars. (A) PCaM WT and N-domain mutants. (B) PCaM WT and C-domain mutants.

EGTA at pH 7.40 and 24 ± 1 °C. Calcium-saturated conditions included 50 mM HEPES, 100 mM KCl, and 5 mM $CaCl_2$ at pH 7.40 and 24 ± 1 °C.

Calcium Titrations. The sequence of PCaM (Figure 1) contains only one Tyr residue (Y138) and no Trp. A calcium-induced increase in fluorescence intensity has been interpreted to indicate a reduced level of quenching in the calcium-saturated state of CaM (*13*) and may be used to monitor calcium binding to sites III and IV, reporting on the average occupancy of those sites {see Figure 2, 1osa; C. Ban, B. Ramakrishnan, K.-Y. Ling, C. Kung, and M. Sundaralingam [http://www.rcsb.org/pdb (*14*)]; see also 1clm (*15*)}. Almost all of the signal may be accounted for by binding calcium to those two sites (*16*, *17*). Although this fluorescence method relies on a single intrinsic spectral reporter group, it agrees with high precision to NMR studies of the properties of the same residue (*17*) and proteolytic footprinting titrations probing other sites in the C-domain [e.g., E87 (*2*) and R106 (*3*)] when identical discontinuous titrations were compared. An SLM-4800 fluorimeter monitored changes in intrinsic Tyr fluorescence (λ_{ex} = 277 nm, λ_{em} = 308 nm) of PCaM (Figure 6) as calcium bound to sites III and IV (*17*). Samples of 1−3 μM PCaM in 50 mM HEPES, 100 mM KCl, 0.5 mM EGTA, and 0.5 mM NTA at pH 7.40 and 22 °C were titrated with 50 mM $CaCl_2$ in the same buffer. The level of free calcium was determined by the degree of saturation of difBAPTA (1−4 μM; λ_{ex} = 257 nm, λ_{em} = 369 nm; K_d = 1.80 μM) as described previously (*17*); 6−12 replicates of each experiment were conducted. The span of fluorescence readings for each titration was normalized to its high and low end points before nonlinear least-squares analysis.

Free Energies of Calcium Binding. The Gibbs free energies of calcium binding to sites III and IV were obtained by fitting the fluorescence-monitored calcium titrations to a model-independent (Adair) equation for binding of ligand to two sites (eq 1). This equation allows the sites within a pair to be nonequivalent (different intrinsic affinities for ligand) and cooperative (interacting). A detailed description of the application of this equation to fluorescence studies of calcium binding to CaM may be found elsewhere (*4*, *17*).

$$Y = \frac{\exp(-\Delta G_1/RT)[X] + 2\exp(-\Delta G_2/RT)[X]^2}{2[1 + \exp(-\Delta G_1/RT)[X] + \exp(-\Delta G_2/RT)[X]^2]} \quad (1)$$

In eq 1, the macroscopic free energy term ΔG_1 represents the sum of the two intrinsic free energies of binding calcium to either site III or site IV (i.e., $\Delta G_1 = \Delta G_{III} + \Delta G_{IV}$). The term ΔG_2 represents the total free energy for binding calcium ([X]) to both sites III and IV (i.e., $\Delta G_2 = \Delta G_{III}\Delta G_{IV}\Delta G_{III-IV}$). The term ΔG_{III-IV} accounts for any positive or negative cooperativity that promotes or penalizes simultaneous occupancy of both sites, regardless of its source or magnitude.

Multiple criteria were used for evaluating the goodness of fit for the parameters that minimized the variance in each fit. These error statistics as reported by nonlin (*18*) included (i) the value of the square root of variance, (ii) the values of asymmetric 65% confidence intervals, (iii) the systematic trends in the distribution of residuals (data not shown), (iv) the magnitude of the span of residuals, and (v) the absolute value of elements of the correlation matrix. Note that application of a more restricted model that required the sites to have identical intrinsic affinities without interactions resulted in a poor fit as measured by the pattern of residuals and the square root of the variance.

It is not possible analytically to determine the intradomain cooperativity, ΔG_c, between sites III and IV from the fluorescence-monitored titration data alone. However, it may be estimated by assuming that binding sites III and IV have equal intrinsic affinities [i.e., $\Delta G_1 = -RT\ln(K_1 = k_{III} + k_{IV} = 2k)$]. Equation 2 gives a lower limit value of cooperative free energy.

$$\Delta G_c = \Delta G_{III-IV} = \Delta G_2 - 2\Delta G_1 - RT\ln(4) \quad (2)$$

Calculated values are reported in Table 2; errors were propagated by nonlin from the resolved uncertainties of ΔG_1 and ΔG_2.

Fractional Populations of Ligation Species. In Figure 7, the fractional populations of liganded species were calculated using the standard equation for the Boltzmann distribution. The probability (f_s) of a single species (s) of a macromolecule is given by eq 3

$$f_s = \frac{\exp(-\Delta G_s/RT)[X]^j}{\sum_{s,j}\exp(-\Delta G_s/RT)[X]^j} \quad (3)$$

where [X] is the ligand activity, ΔG_s represents the Gibbs free energy [$-RT\ln(K_s)$] of species s, and j represents the

Table 2: Gibbs Free Energies of Calcium Binding to Sites III and IV of PCaM

protein	ΔG_1[a]	ΔG_2	SD	ΔG_c[b]
rat CaM WT	-7.26 ± 0.15	-15.4 ± 0.05	0.010	-1.68 ± 0.30
PCaM WT	-7.38 ± 0.25	-16.2 ± 0.05	0.014	-2.27 ± 0.50
V35I/D50N	-7.64 ± 0.29	-16.2 ± 0.08	0.025	-1.75 ± 0.58
G40E	-7.51 ± 0.25	-16.4 ± 0.05	0.017	-2.21 ± 0.47
G40E/D50N	-7.21 ± 0.16	-16.0 ± 0.03	0.009	-2.36 ± 0.33
D50G	-7.44 ± 0.37	-16.3 ± 0.07	0.024	-2.18 ± 0.73
E54K	-7.40 ± 0.25	-16.2 ± 0.06	0.019	-2.17 ± 0.59
G59S	-7.64 ± 0.29	-16.3 ± 0.08	0.023	-1.81 ± 0.58
average[c]		-16.2 ± 0.15		
D95G	-6.97 ± 0.06	-13.5 ± 0.05	0.013	-0.35 ± 0.15
S101F	-6.86 ± 0.07	-13.8 ± 0.05	0.014	-0.93 ± 0.17
E104K	-7.36 ± 0.04	-13.7 ± 0.05	0.010	0.18 ± 0.06
H135R	-6.52 ± 0.21	-14.2 ± 0.05	0.014	-1.95 ± 0.40
I136T	-7.44 ± 0.10	-13.1 ± 0.18	0.025	0.95 ± 0.19
average[d]		-13.7 ± 0.44		
M145V	-7.51 ± 0.21	-15.9 ± 0.06	0.018	-1.71 ± 0.39

[a] Gibbs free energies are fit according to eq 1; units of kilocalories per mole (1 kcal = 4.184 J). To overestimate the uncertainty in fitted values, the greater of the positive or negative limit of each asymmetric 65% confidence interval was tabulated. [b] The estimate of cooperative free energy was calculated by eq 2, and errors were propagated by nonlin; this formulation provides a lower limit for the value of actual cooperativity. [c] Average of ΔG_2 for six N-domain mutants. [d] Average of ΔG_2 for five C-domain mutants (not including M145V).

stoichiometry of ligand(s) binding to species s. Each free energy term (ΔG_s) is the sum of the intrinsic and cooperative interactions that apply to that species. The denominator of this expression is Z, the binding polynomial for the macromolecule.

A general partition function for describing the 16 possible species of CaM required four intrinsic equilibrium constants ($k_I - k_{IV}$) for calcium binding to each of the EF-hand sites, at least two intradomain cooperativity terms (k_{I-II} and k_{III-IV}) and an interdomain cooperativity term (k_{N-C}). On the basis of studies of rat CaM (*16*) and PCaM (Table 2), the properties of WT PCaM may be approximated by the following relationships: $k_I = k_{II}$ ($\Delta G_I = \Delta G_{II} = -6.5$ kcal/mol), $k_{III} = k_{IV}$ ($\Delta G_{III} = \Delta G_{IV} = -7.0$ kcal/mol), $k_{I-II} = k_{III-IV}$ ($\Delta G_{I-II} = \Delta G_{III-IV} = -2.0$ kcal/mol), and $\Delta G_{N-C} = 2.0$ kcal/mol. In the formulation of the partition function, the free energy of any species having site I or II occupied included ΔG_{N-C}, the interdomain cooperativity term. Specifically, Z equals $[1 + (k_I k_{N-C} + k_{II} k_{N-C} + k_{III} + k_{IV})[X] + (k_I k_{II} k_{I-II} k_{N-C} + k_I k_{III} k_{N-C} + k_I k_{IV} k_{N-C} + k_{II} k_{III} k_{N-C} + k_{II} k_{IV} k_{N-C} + k_{III} k_{IV} k_{III-IV})[X]^2 + (k_I k_{II} k_{III} k_{I-II} k_{N-C} + k_{III} k_{IV} k_{III-IV} k_I k_{N-C} + k_{III} k_{IV} k_{III-IV} k_{II} k_{N-C} + k_I k_{II} k_{I-II} k_{IV} k_{N-C})[X]^3 + k_I k_{II} k_{III} k_{IV} k_{I-II} k_{III-IV} k_{N-C}[X]^4]$. The individual states are represented by a linear array of four digits according to the pattern of vacancy (0) or occupancy (1) of each of the four sites (e.g., apo PCaM is [0000], whereas PCaM with sites III and IV occupied is [0011]).

RESULTS

The major goal of this study was to determine whether all of the mutants could bind calcium and undergo conformational changes similar to those of wild type PCaM. Spectroscopic and hydrodynamic properties of wild type PCaM were compared to those of the apo and calcium-saturated end states of each of the 12 mutants. Calcium titrations were monitored by changes in intrinsic tyrosine fluorescence to determine whether the mutations affected calcium binding to sites III and IV.

UV Spectra. The calcium-dependent UV spectra of wild-type PCaM shown in Figure 3 were characteristic of those for all 12 of the mutants (data not shown). The distinctive fine structure below 280 nm reflects the lack of tryptophan and the 8:1 Phe:Tyr ratio. For all mutants, the absorbance at 280 nm decreased upon calcium binding as is characteristic of vertebrate calmodulin sequences (*16*). These spectra indicated that a saturating level of calcium was able to induce a conformational change in all of the PCaM mutants.

Secondary Structure. To explore the nature of the calcium-induced conformational change, circular dichroism was used to monitor secondary structure. The characteristic difference between apo and calcium-saturated CaM that has been reported for vertebrate CaM (for a review, see ref *16*) was observed for wild type PCaM. Calcium saturation induced an average decrease of 12.2% in ellipticity at 222 nm ($\Delta\theta_{222}$), indicating greater order (more regions of persistent helix throughout the sequence of the protein) or changes in helix orientation in the calcium-saturated form.

For all 12 of the mutants (Table 1), calcium saturation caused the value of θ_{222} to change in the same direction as that of wild type PCaM, indicating that all of the mutants undergo calcium-induced conformational switching. However, the quantitative extent of change in θ_{222} differed depending on the site of mutation. For each protein in the set of six N-domain mutants, the fractional change in ellipticity ($\Delta\theta_{222}$) was within 2% of the wild type value of 12.2%. Values of $\Delta\theta_{222}$ for four of the six C-domain mutants were similarly close to that of wild type. Notably, however, the value of $\Delta\theta_{222}$ for E104K PCaM was much smaller (7.2%), while the value for I136T PCaM was much larger (33.0%).

Hydrodynamic Properties. Measurements of calcium-induced changes in ellipticity demonstrated the ability of the mutant proteins to undergo changes in secondary structure similar to those of wild type PCaM. However, the values of $\Delta\theta_{222}$ in Table 1 do not indicate whether concomitant changes in tertiary structure also occur. To assess whether the molecular dimensions of the hydrated apo or calcium-saturated forms of these mutants were affected, we determined the Stokes radius (R_s) of each using analytical gel permeation chromatography. Figure 5 shows the average values determined for each of the mutants.

For all of the proteins, the Stokes radii of both the apo and calcium-saturated forms were much larger than the value of 18.3 Å which is predicted for a globular protein with the same molecular weight. This discrepancy has been observed for rat CaM under identical conditions (*4*) and may be explained by the elongated shape of CaM. Analytical ultracentrifugation studies (J.-T. Eppel and M. A. Shea, unpublished) indicate that wild type PCaM is a monomer in both the apo and calcium-saturated forms at the concentrations used in this study.

Like the behavior of rat CaM, calcium binding caused the value of R_s to decrease for wild type PCaM and all of the mutants (Table 1). Analysis of the averages and standard deviations of the R_s values showed that the distribution of values for the apo conformations [standard deviation (SD) = 0.57 Å] was twice as large as that of the calcium-saturated forms (SD = 0.23 Å). This indicates greater heterogeneity in the apo conformations.

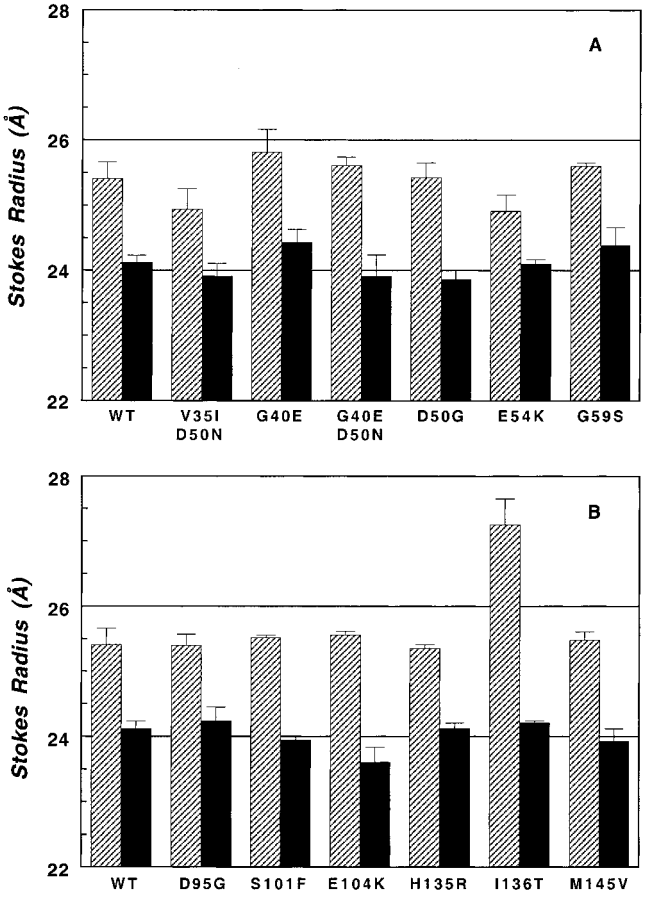

FIGURE 5: Stokes radii under apo (hatched) and calcium-saturating (black) conditions. (A) PCaM WT and N-domain mutants. (B) WT and C-domain mutants. Apo conditions were 50 mM HEPES, 100 mM KCl, 0.5 mM NTA, and 0.5 mM EGTA at pH 7.40 and 24 ± 1 °C. Calcium saturating conditions were the same except 5 mM $CaCl_2$ was substituted for EGTA and NTA.

The difference between the Stokes radii of apo and calcium-saturated wild type PCaM (ΔR_s) was 1.29 Å. As shown in Table 1 for the apo proteins, values of ΔR_s ranged from 0.81 Å (for E54K PCaM) to 3.04 Å (for I136T PCaM) which is 2 Å larger than that of apo wild type PCaM. With the exception of data for E104K PCaM, variations in the values of ΔR_s for individual mutants were linearly correlated with values of $\Delta\theta_{222}$ (plot not shown). The R_s of the apo form of two of the mutants (V35I/D50N and E54K) is slightly smaller than that of the wild type protein.

Calcium Titrations. Calcium titrations (Figure 6) monitored by measuring changes in the intrinsic tyrosine fluorescence of Y138 in site IV afford an opportunity to determine the average calcium binding properties of sites III and IV in the C-domain of PCaM. In wild type calmodulin from many species, most of the enhancement in fluorescence intensity of Y138 arises from calcium binding to those two high-affinity sites with only a small contribution from sites I and II. Calcium binding to all of the PCaM mutants resulted in fluorescence enhancements that were similar in magnitude to that of wild type.

Titrations of wild type PCaM yielded a total free energy (ΔG_2) of calcium binding of −16.2 kcal/mol (Table 2). Under the same conditions, the affinity of rat CaM (representative of CaM from vertebrate species) was less favorable by 0.8 kcal/mol, a significant difference given the experimental precision (0.05 kcal/mol) of these studies.

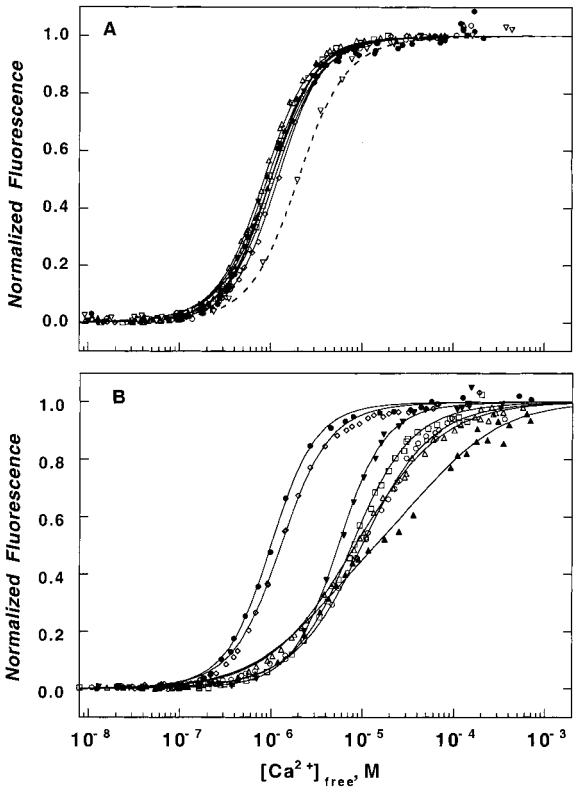

FIGURE 6: Calcium binding to sites III and IV monitored by the fluorescence of Y138. (A) PCaM WT (●) and N-domain mutants (□) V35I/D50N, (△) G40E, (▼) G40E/D50N, (▲) D50G, (◇) E54K, and (◊) G59S and (▽) rat CaM WT. (B) PCaM WT (●) and C-domain mutants (○) D95G, (□) S101F, (△) E104K, (▼) H135R, (▲) I136T, and (◇) M145V.

The calcium binding properties of sites III and IV in the six PCaM mutants altered only in the N-domain (Figure 6A) exhibited no significant difference from wild type PCaM. The ΔG_2 values ranged from −16.0 to −16.4 kcal/mol, with an average of −16.23 kcal/mol. For all of these proteins, the estimated value of ΔG_c was close to −2 kcal/mol. This was also the case for M145V PCaM, the only one of the class of mutations of the C-domain to be located in a region outside of the 12-residue calcium binding sites (see boxed regions of Figure 1). Its value of ΔG_2 was estimated as −15.9 kcal/mol, nearly identical to that of G40E/D50N PCaM and very close to that of the wild type. The estimated free energy of cooperativity was also nearly identical to that of the wild type.

The titrations of the other five C-domain mutants (those containing mutations within sites III or IV) exhibited significant decreases in their binding affinity compared to that of wild type PCaM (Figure 6B). The average value of ΔG_2 for these five mutants was −13.7 ± 0.4 kcal/mol, approximately 2.5 kcal/mol less favorable than that of the wild type. The estimates of ΔG_c for these five proteins varied significantly, from −1.95 kcal/mol (i.e., positive cooperativity similar to that of the wild type protein) for H135R PCaM to 0.95 kcal/mol (anticooperativity) for I136T PCaM.

Simulations of Probability Distributions. Changes in calcium affinity and cooperativity affect both the free calcium concentration required to reach saturation and the pathway taken. At any specific pCa, the relative abundance of intermediate species will affect the efficiency of target activation. To demonstrate how the energetic differences

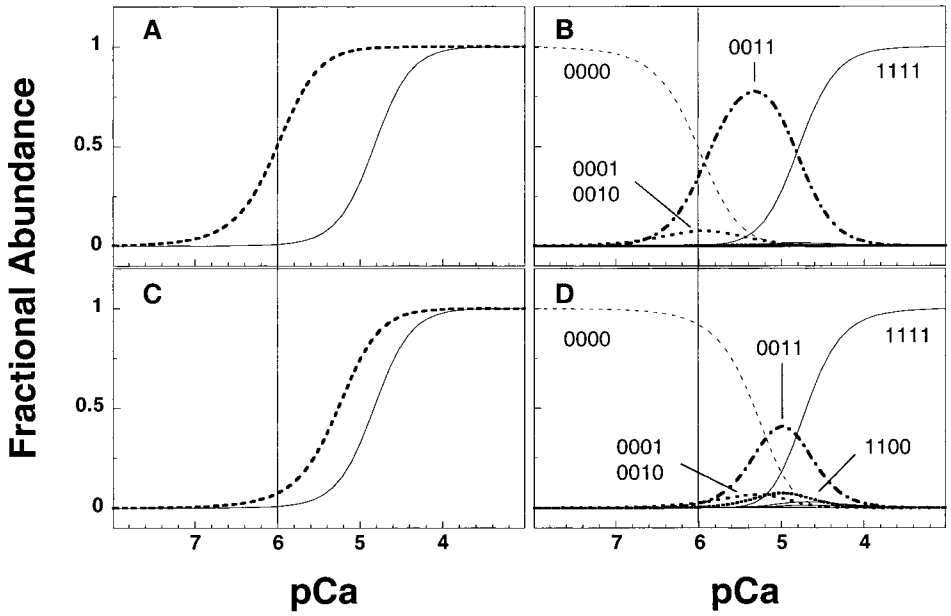

FIGURE 7: Calcium-dependent distribution of ligation species of CaM. (A and C) Fractional abundance of species having site I, site II, or both occupied (solid curve) and species having site III, site IV, or both occupied (dashed curve). (A) Wild type PCaM. (C) H135R-like mutant in which energies ΔG_{III} and ΔG_{IV} were both reduced by 1 kcal/mol. (B and D) Abundance of all 16 ligation species. (B) Wild-type PCaM. (D) H135R-like mutant. See Materials and Methods for values of binding free energies used in simulations.

listed in Table 2 would affect the functional properties of CaM, probability distributions were simulated for two representative but idealized cases (all energies were assigned integer or half-integer values).

For the wild type case (panels A and B of Figure 7) CaM makes a sequential transition from zero to two to four calcium ions. Figure 7A shows that when the abundance of species having one or both sites of the C-domain occupied surpasses 92%, species having one or both sites in the N-domain occupied comprised only 7% of the total population (a ratio of ~13:1). Figure 7B shows that the major intermediate populated between apo ([0000]) and holo (four ligands, [1111]) PCaM was the species with both sites III and IV occupied; its maximal abundance was 78%. The two singly liganded species with either site III or site IV occupied reached a maximum of less than 8% each. The other 11 intermediates were never populated to an extent greater than 3% of the total. Thus, the PCaM calcium-binding pathway operates by filling sites III and IV almost completely before occupying sites I or II, consistent with vertebrate CaM.

In panels C and D of Figure 7, corresponding simulations are shown for a "C-domain mutant" in which the intrinsic binding energy of both high-affinity sites (III and IV) was made less favorable by 1 kcal/mol but cooperativity energies were preserved. These values mimic the properties that are known so far for a mutant such as H135R PCaM. Comparison of the occupancy of the C-domain at a micromolar free calcium level (pCa 6, panels A and C of Figure 7) reflects the effect of the loss of −2 kcal/mol in binding energy. Furthermore, the domains no longer saturate sequentially. When species having sites III or IV filled comprise 91% of the total, species having site I or II filled comprise 62% of the total population (a ratio of ~1.5:1, a factor of 10 lower than the wild type case). Figure 7D shows that although the most abundant intermediate was the doubly liganded species with sites III and IV occupied ([0011]), as it had been for the wild type protein (Figure 7B), its maximal value was reduced to 41% (vs 78% for wild type PCaM) and it peaked at a much higher level of calcium. Three other intermediates were populated at levels greater than 3%. These included the species having site III or IV occupied ([0010] and [0001]) and the species with both sites I and II occupied ([1100]).

DISCUSSION

The studies reported here focused on exploring the molecular basis of faulty calcium activation of two sets of *Paramecium* CaM mutants that are defective in regulating ion channels (*8*, *9*). The structural basis for the interactions between CaM and these ion channels is not well characterized. The major goal of this study was to determine whether these mutants responded to calcium in a manner that is structurally and thermodynamically similar to wild type PCaM in the absence of target proteins. From this behavior, we may infer some elements of the mechanisms of target activation that are faulty in these mutants.

Structures of Apo and Calcium-Saturated Species. All of the mutants can bind calcium and adopt a calcium-saturated conformation similar to that of wild type PCaM as judged by changes in the environment of aromatic amino acids (Figures 3 and 6), secondary structure (Figure 4), and hydrodynamic behavior (Figure 5) which reflects macroscopic properties of tertiary structure.

As seen in Table 1, the Stokes radius of wild type PCaM decreased slightly (by 1.3 Å) upon calcium binding as had been observed for rat CaM (*7*). The magnitude of change (ΔR_s) was close to 1 Å for most of the mutants. However, the I136T mutation (located in the β-sheet that pairs sites III and IV) caused the apo end state to be much larger than normal (Figure 5). Its molar ellipticity (data not shown) and calcium-induced $\Delta\theta_{222}$ (Figure 4) indicated that I136T PCaM is much less ordered than the wild type, consistent with studies of a similar mutant of *Drosophila* CaM [V136T (*19*)]. We expect that the apo C-domain of this mutant has little residual structure (i.e., it is like a molten globule).

Data reported in Table 1 show a linear correlation between ΔR_s and $\Delta\theta_{222}$ measured for wild type and 11 of the mutants (the exception is E104K PCaM). The hydrated size of the PCaM mutants decreased in proportion to the calcium-induced increase in helicity concomitant with the opening of the hydrophobic cleft in each domain. This correlation does not necessarily mean that the end-to-end length of the protein molecule is smaller. Small-angle X-ray scattering studies of vertebrate CaM showed a small increase in the radius of gyration (R_g) ranging from 0.1 (*20*) to 2.5 Å (*21*) upon binding calcium, and the maximum dimension between two atoms (d_{max}) in CaM increased by a range from 4 (*20*, *22*) to 5 Å (*23*, *24*). Since R_s reports on hydrated dimensions while R_g does not, the difference between these parameters may be rationalized if there is a significant release of water upon calcium binding to CaM (*25*).

Calcium Binding to Sites III and IV. As shown in Figure 6 for wild type PCaM and 12 mutants, calcium binding induced an increase in the fluorescence intensity of Y138 located in site IV **(**Figure 2). The mutations in helices B and C (in the N-domain) do not perturb the calcium-induced response of Y138, indicating that the average calcium binding properties of sites III and IV are identical to those of the wild type. Although it is possible that there are conformational changes within the C-domain that are not detected by fluorescence, the simplest conclusion is that calcium binding affinities of sites in the C-domain are unaffected by these mutations in the N-domain.

As shown in Figure 6B, all of the mutations within sites III and IV in the C-domain have a significant effect on calcium affinity. There is a wide distribution of changes in the total free energy and cooperativity of binding as listed in Table 2. However, all of these mutants show an offset in the absolute level of free calcium required to reach 50% saturation of the C-domain. Most will require 100 μM free calcium (pCa 4) or more to reach 90% saturation. Thus, it is questionable whether transient increases in cellular levels of calcium will be sufficient to trigger conformational changes of the C-domain that are necessary for target activation.

Cooperativity. The I136T mutation has the most deleterious effects on conformational properties and occurs at position 8 in binding site IV, a position implicated in intradomain cooperativity for all paired EF-hand binding sites (*19*). Thus, its effect on C-domain cooperativity was expected. Notably, mutations S101F and H135R which occur at position 7 in their respective binding loops had little or no effect on cooperativity (Table 2). This is consistent with the view that the backbone carbonyl atom at position 7 chelates the cation, while the side chain at position 8 promotes interactions between sites (*19*, *26*).

It should be emphasized that in the calculation of the intradomain cooperativity for all of the proteins having mutations within site III or IV (i.e., five of the six mutants in the set of C-domain mutants), the assumption that the two binding sites were equivalent in binding affinity may not apply. However, the calculated values of ΔG_c are lower limits (see the discussion in ref *17*) and serve to underscore the fact that the wild type (positive) cooperative interactions have been drastically disrupted in these mutants. The values of ΔG_c also highlight the difference between these titrations and those for the comparable studies of M145V PCaM and the six mutants altered in the N-domain.

Interdomain interactions cannot be resolved from the experimental results reported here and will await analysis by two-dimensional NMR and proteolytic footprinting of discontinuous equilibrium titrations (*27*).

Comparison to Vertebrate CaM. Sites III and IV of PCaM had a higher affinity (1 kcal/mol) than those sites in rat CaM (Table 2). Of the 17 differences between the two sequences, only four are located within the 24 residues that comprise binding loops III and IV (Figure 1). Several of the differences (e.g., V vs I at position 136) represent natural variation found in calmodulin from many eukaryotes. This suggests that differences found within helices E−H are also important for determining calcium affinity. It remains to be seen whether PCaM has the same affinity at sites I and II as vertebrate CaM; only four residues differ between the N-domain regions of the two sequences. Kung and co-workers demonstrated that bovine CaM did not restore the wild type phenotype to *Paramecium* cells with a CaM mutation (*28*), but whether this was because of differences in calcium affinity or contacts between CaM and its targets is not known.

Conformational Switching. The PCaM mutants differ from the wild type protein in their inability to activate sodium or potassium channels depending on the domain that is mutated (*29*). However, hydrodynamic and spectroscopic studies reported here show that most of the mutants are able to adopt conformations similar to those of wild type PCaM in both the apo and calcium-saturated states. Thus, the mutations do not destroy CaM but very selectively disarm it.

The six N-domain mutants underwent normal calcium-induced conformational switching as measured by changes in ellipticity and hydrated radius. It is possible that these mutants are defective in ion channel regulation solely because they no longer make all of the surface contacts that are necessary for association with target proteins. On the basis of known structures of CaM bound to target molecules, the residues affected in two of them (V35I/D50N and E54K) are expected to participate in CaM−target contacts directly (*30*−*32*). Because all six mutants bind calcium normally at sites III and IV, this suggests that retention of wild type conformational properties of the C-domain is not sufficient for activation of the affected *Paramecium* sodium channel. Thus, it is essential to determine whether there are differences in calcium binding at sites I and II as well as differences in protein interfaces.

As shown in Figure 6B, M145V PCaM [with a mutation in helix H, in a "methionine puddle" (*33*)] differs dramatically from the other five mutants of the C-domain in that it binds calcium to sites III and IV in a manner very similar to that of wild type PCaM. Figures 4 and 5 show that calcium triggers normal conformational changes in M145V PCaM. Mutation of methionine to valine would affect both the length and unique conformational flexibility of the side chain. Although it is a formal possibility that this mutation may alter calcium binding properties in the presence of the physiological target molecule, it is more likely that it interferes with proper target interactions directly. Atomic resolution structures of CaM−peptide complexes (e.g., CaM bound to a peptide from MLCK, CaMKII, CaMKK, or calcium-ATPase) exhibit interactions between M145 and the target region (*30*−*32*). It is known that methionines in the C-domain of CaM affect the affinity of CaM for calcium-ATPase (*6*) and have different susceptibilities for oxidation

in vivo and in vitro (*34*, *35*). Thus, we infer that the primary defect of M145V PCaM is modification of target association and/or activation rather than calcium affinity.

Properties of the PCaM variants with differences within site III or IV suggest that their phenotypic defects result from changes in the transition between the apo and holo end states. Simulations of the abundance of individual ligation species (Figure 7) showed that a loss of 2 kcal/mol of intrinsic binding free energy in the C-domain (e.g., as observed for H135R PCaM) was sufficient to change both the concentration dependence of domain saturation (Figure 7C) and the relative abundance of intermediate species (Figure 7D). The small separation between the curves representing the occupancy of each domain of a mutant (Figure 7C) may be diminished further if the energetics of sites I and II are altered as well.

Other C-domain mutants that exhibited a reduction in intradomain cooperativity as well as intrinsic binding affinity would be affected even more severely, requiring a higher level of calcium for complete saturation and having a more heterogeneous population of intermediate species. The physiological implications of changes in the distribution of intermediate states would vary depending on whether the regulation of a particular channel required interactions with only one or both domains of CaM and whether the wild type order of filling the domains (C-domain before N-domain) was significant for both association and activation of the target.

Target Association and Activation. Many atomic models of Ca^{2+}_4−CaM−peptide co-complexes show noncovalent interactions to be similar in number and kind with both domains of CaM contacting the target (*31*). However, either orientation of the target is possible. For example, CaMKK interacts with both domains of Ca^{2+}_4−CaM but does so in a domain-dependent fashion that is opposite than that seen for MLCK and CaMKII (*30*). Although many target proteins associate preferentially with calcium-saturated CaM (*36*) and are activated by interacting extensively with both domains of that molecular species, there would be no channel-specific regulatory mutants of PCaM if that were the only possible route to CaM-dependent regulation. In other words, all of these mutants should have been observed to affect both sodium and potassium channels equally if that were the case. This argues for regulatory roles for some of the other 15 states.

There is mounting evidence that some targets do bind to the apo or partially saturated species of CaM. Neuromodulin associates preferentially with apo CaM and is released by calcium binding (*37*). CaM in both its apo and calcium-saturated forms associates with SK potassium channels (*38*, *39*), L-type calcium channels (*40*, *41*), the tetrameric ryanodine receptor (*42*), and phosphorylase kinase (*43*). Presumably, intermediate species remain associated with these targets during the transition from zero to four calcium ions bound to CaM. Partially saturated CaM intermediates also may regulate targets (*38*−*40*, *44*−*46*). It is possible for a single domain of full-length CaM to interact preferentially with a target or antagonist. Examples include the C-domain of Ca^{2+}_4−CaM interacting with a single TFP molecule (*47*) or a peptide from calcium-ATPase (*32*). Regulation may be domain-dependent in a fashion opposite from that seen for PCaM [e.g., mutations in sites I and II of vertebrate CaM selectively prevent calcium-dependent activation of the SK potassium channel (*39*)]. In a kinetic model of target activation by CaM, the calcium-saturated C-domain associates with the target followed by binding of the calcium-saturated N-domain to the target (*48*).

The apo and calcium-saturated forms of the majority of the PCaM mutants reported here are similar to wild type PCaM. The fact that the mutants are defective in channel activation suggests several possibilities. Some may never reach the required end state at physiological calcium levels because of decreases in calcium affinity. Interactions between a target and one domain of PCaM may be necessary and sufficient for activation, but the isolated mutations severely diminish the extent of association with and activation of the target. If the order of saturating the sites of PCaM is the key regulatory feature, an increased abundance of species with the N-domain saturated and capable of binding the target would poison the pool of CaM−target heterodimers with nonproductive co-complexes. Evidently, the complexity of orchestrating the transition through 14 intermediate states allows the collection of PCaM mutants to utilize several different paths that diverge from normal but are still viable. To fully understand how PCaM activates ion channels in *Paramecium*, it will be necessary to determine whether there is direct binding, building on previous studies (*49*, *50*). Then, it will be essential to distinguish between the molecular mechanisms of association and activation per se.

Summary. In eukaryotic organisms, cooperative calcium binding to the two EF-hand (helix−loop−helix) sites in each of the two domains of calmodulin (see Figure 1) drives conformational changes that enable it to regulate its target proteins. Although the domains are very similar in primary structure, they have a 10-fold difference in calcium affinity. Identified mutations in the N-domain of PCaM that affect sodium channel activation do not compromise potassium channel activation and vice versa for the set of identified mutations in the C-domain (*29*). Therefore, the behavior of these proteins is not consistent with models in which both domains of CaM are equivalent partners in the activation of all CaM target proteins. Although these mutations disrupt pathways of binding and linkage in the PCaM sequence, they are able to bind calcium and can be driven to undergo conformational changes consistent with the behavior of the wild type protein. Therefore, the physiological defects may be traced to differences in the properties of the 14 intermediate states of CaM (i.e., those molecules partially saturated with calcium) or the contacts made with target proteins. Further analysis of the coupling between calcium binding and conformations of the intermediate states of these mutants in the presence of target peptides or drugs will contribute to understanding pathways of conformational change and the roles these residues play in signal transduction. They will also help us to understand how similar domains can evolve to have separate functions in a highly conserved eukaryotic protein.

ACKNOWLEDGMENT

We thank Ching Kung and co-workers at the University of Wisconsin for generously sharing their bacterial overexpression vectors for *Paramecium* CaM and the 12 mutants used in this study. We thank our colleagues Laurel Coffeen,

Maria Hutchins, Cynthia Kephart, and Mark Yates for technical assistance with protein purification and significant preliminary studies of subsets of these mutants. The University of Iowa College of Medicine Molecular Analysis Facility provided amino acid analyses.

REFERENCES

1. Klevit, R. E., Dalgarno, D. C., Levine, B. A., and Williams, R. J. P. (1984) *Eur. J. Biochem. 139*, 109−114.
2. Pedigo, S., and Shea, M. A. (1995) *Biochemistry 34*, 1179−1196.
3. Shea, M. A., Verhoeven, A. S., and Pedigo, S. (1996) *Biochemistry 35*, 2943−2957.
4. Sorensen, B. R., and Shea, M. A. (1998) *Biochemistry 37*, 4244−4253.
5. Weinstein, H., and Mehler, E. L. (1994) *Annu. Rev. Physiol. 56*, 213−236.
6. Yin, D., Sun, H., Weaver, R. F., and Squier, T. C. (1999) *Biochemistry 38*, 13654−13660.
7. Sorensen, B. R., and Shea, M. A. (1996) *Biophys. J. 71*, 3407−3420.
8. Kung, C., Preston, R. R., Maley, M. E., Ling, K.-Y., Kanabrocki, J. A., Seavey, B. R., and Saimi, Y. (1992) *Cell Calcium 13*, 413−425.
9. Saimi, Y., and Kung, C. (1994) *FEBS Lett. 350*, 155−158.
10. Ohya, Y., and Botstein, D. (1994) *Science 263*, 963−966.
11. Ohya, Y., and Botstein, D. (1994) *Genetics 138*, 1041−1054.
12. Putkey, J. A., Slaughter, G. R., and Means, A. R. (1985) *J. Biol. Chem. 260*, 4704−4712.
13. Sun, H., Yin, D., and Squier, T. C. (1999) *Biochemistry 38*, 12266−12279.
14. Berman, H. M., Westbrook, J., Feng, Z., Gilliland, G., Bhat, T. N., Weissig, H., Shindyalov, I. N., and Bourne, P. E. (2000) *Nucleic Acids Res. 28*, 235−242.
15. Rao, S. T., Wu, S., Satyshur, K. A., Ling, K.-Y., Kung, C., and Sundaralingam, M. (1993) *Protein Sci. 2*, 436−447.
16. Klevit, R. E. (1983) *Methods Enzymol. 102*, 82−104.
17. Pedigo, S., and Shea, M. A. (1995) *Biochemistry 34*, 10676−10689.
18. Johnson, M. L., and Frasier, S. G. (1985) *Methods Enzymol. 117*, 301−342.
19. Browne, J. P., Strom, M., Martin, S. R., and Bayley, P. M. (1997) *Biochemistry 36*, 9550−9561.
20. Heidorn, D. B., and Trewhella, J. (1988) *Biochemistry 27*, 909−915.
21. Yoshino, H., Wakita, M., and Izumi, Y. (1993) *J. Biol. Chem. 268*, 12123−12128.
22. Seaton, B. A., Head, J. F., Engelman, D. M., and Richards, F. M. (1985) *Biochemistry 24*, 6740−6743.
23. Kataoka, M., Head, J. F., Seaton, B. A., and Engelman, D. M. (1989) *Proc. Natl. Acad. Sci. U.S.A. 86*, 6944−6948.
24. Kataoka, M., Head, J. F., Persechini, A., Kretsinger, R. H., and Engelman, D. M. (1991) *Biochemistry 30*, 1188−1192.
25. Kupke, D. W., and Dorrier, T. E. (1986) *Biochem. Biophys. Res. Commun. 138*, 199−204.
26. Strynadka, N. C. J., and James, M. N. G. (1989) *Annu. Rev. Biochem. 58*, 951−998.
27. Shea, M. A., Sorensen, B. R., Pedigo, S., and Verhoeven, A. (2000) *Methods Enzymol. 323*, 254−301.
28. Hinrichsen, R. D., Burgess-Cassler, A., Soltvedt, B. C., Hennessey, T., and Kung, C. (1986) *Science 232*, 503−506.
29. Kink, J. A., Maley, M. E., Preston, R. R., Ling, K.-Y., Wallen-Friedman, M. A., Saimi, Y., and Kung, C. (1990) *Cell 62*, 165−174.
30. Osawa, M., Tokumitsu, H., Swindells, M. B., Kurihara, H., Orita, M., Shibanuma, T., Furuya, T., and Ikura, M. (1999) *Nat. Struct. Biol. 6*, 819−824.
31. Crivici, A., and Ikura, M. (1995) in *Annual Review of Biophysics and Biomolecular Structure* (Stroud, R. M., Ed.) pp 85−116, Annual Reviews Inc., Palo Alto, CA.
32. Elshorst, B., Hennig, M., Försterling, H., Diener, A., Maurer, M., Schulte, P., Schwalbe, H., Griesinger, C., Krebs, J., Schmid, H., Vorherr, T., and Carafoli, E. (1999) *Biochemistry 38*, 12320−12332.
33. O'Neil, K. T., and DeGrado, W. F. (1990) *Trends Biochem. Sci. 15* (2), 59−64.
34. Gao, J., Yin, D. H., Yao, Y., Sun, H., Qin, Z., Schöneich, C., Williams, T. D., and Squier, T. C. (1998) *Biophys. J. 74*, 1115−1134.
35. Gao, J., Yin, D., Yao, Y., Williams, T. D., and Squier, T. C. (1998) *Biochemistry 37*, 9536−9548.
36. Olwin, B. B., and Storm, D. R. (1985) *Biochemistry 24*, 8081−8086.
37. Andreasen, T. J., Luetje, C. W., Heideman, W., and Storm, D. R. (1983) *Biochemistry 22*, 4615−4618.
38. Xia, X. M., Fakler, B., Rivard, A., Wayman, G., Johnson-Pais, T., Keen, J. E., Ishii, T., Hirschberg, B., Bond, C. T., Lutsenko, S., Maylie, J., and Adelman, J. (1998) *Nature 395*, 503−507.
39. Keen, J. E., Khawaled, R., Farrens, D. L., Neelands, T., Rivard, A., Bond, C. T., Janowsky, A., Fakler, B., Adelman, J. P., and Maylie, J. (1999) *J. Neurosci. 19*, 8830−8838.
40. Zühlke, R. D., Pitt, G. S., Deisseroth, K., Tsien, R. W., and Reuter, H. (1999) *Nature 399*, 159−162.
41. Ehlers, M. D., and Augustine, G. J. (1999) *Nature 399*, 107−108.
42. Moore, C. P., Rodney, G., Zhang, J. Z., Santacruz-Toloza, L., Strasburg, G., and Hamilton, S. L. (1999) *Biochemistry 38*, 8532−8537.
43. Picton, C., Shenolikar, S., Grand, R., and Cohen, P. (1983) *Methods Enzymol. 102*, 219−227.
44. Klee, C. B., Newton, D. L., Ni, W. C., and Haiech, J. (1986) in *Calcium and the Cell* (Evered, D., and Whelan, J., Eds.) pp 162−182, John Wiley and Sons, New York.
45. Persechini, A., White, H. D., and Gansz, K. J. (1996) *J. Biol. Chem. 271*, 62−67.
46. Mirzoeva, S., Weigand, S., Lukas, T. J., Shuvalova, L., Anderson, W. F., and Watterson, D. M. (1999) *Biochemistry 38*, 3936−3947.
47. Cook, W. J., Walter, L. J., and Walter, M. R. (1994) *Biochemistry 33*, 15259−15265.
48. Brown, S. E., Martin, S. R., and Bayley, P. M. (1997) *J. Biol. Chem. 272*, 3389−3397.
49. Kubalski, A., Martinac, B., and Saimi, Y. (1989) *J. Membr. Biol. 112*, 91−96.
50. Saimi, Y., and Martinac, B. (1989) *J. Membr. Biol. 112*, 79−89.
51. Kraulis, P. J. (1991) *J. Appl. Crystallogr. 24*, 946−950.

BI000037W